Engineering and Technology Journal
Journal homepage: engtechjournal.org

Multi-Objective Optimization of Friction Stir Welding for Aluminum Alloy (2024-T3)

Abbas K. Hussein [a], Laith K. Abbas [b], Ahmed A. Seger [c*]

[a] Head of Nano-Technology Center, University of Technology, Baghdad, Iraq. abbas2000x@gmail.com.

[b] Department of Materials Engineering, University of Technology, Baghdad, Iraq. laithka2012@gmail.com.

[c] Department of Materials Engineering, University of Technology, Baghdad, Iraq. ahmedseger90@gmail.com.

*Corresponding author.

Submitted: 24/05/2019 Accepted: 31/07/2019 Published: 25/02/2020

K E Y W O R D S

AA2024-T3, FSW process, tensile strength, Taguchi, Fuzzy Logic, multi-response.

A B S T R A C T

In this research, a multi-response optimization based on Taguchi method is proposed for friction stir welding (FSW) process for (2024-T3) aluminum alloy. Three different shoulder diameters of tools with tapered pin geometry of (12, 14 and 14 mm) with variable rotation speed (710, 1000 and 1400 rpm) and welding speed of (40, 56 and 80 mm/min), three different tilting angles of (1, 2 and 3 degree) and three welding direction of (1, 2 and 3 passes). The results of this work showed the single optimization by using (Taguchi method) at the optimum condition for the tensile strength and yield strength were (365 MPa) and (258 MPa) respectively; at the parameters: shoulder diameter (14 mm), rotation speed (1400 rpm), linear speed (40 mm/min), tilting angle ((3°) for tensile strength and (1°) for yield strength) and welding direction (3 passes). The results of multi-response optimization for (FSW) process at the optimum condition for tensile strength and yield strength were (371 MPa) and (268 MPa), respectively; at the parameters: shoulder diameter (14 mm), rotation speed (1400 rpm), linear speed (40 mm/min), tilting angle (3°) and welding direction (3 passes).

How to cite this article: A.K. Hussein, L.K. Abbas and A.A. Seger, "Multi-objective optimization of friction stir welding for aluminum alloy (2024-T3)," Engineering and Technology Journal, Vol. 38, Part A, No. 02, pp. 185-198, 2020.

DOI: https://doi.org/10.30684/etj.v38i2A.280

1. Introduction

Some alloys of aluminum are not considered weldable by commercial methods and are generally used with riveted construction. The most extensive application of these alloys such as (2xxx) alloys usually has been in the aircraft industry [1-3]. Friction stir welding can be used as a solid-state welding to join aluminum sheets and plates without any filler wire or shielding gas use. All series of aluminum alloys have been successfully friction stir welded [4-6]. The aluminum alloys of (2xxx) series are practically unwedable because the formation of aluminum-copper intermetallic in weld metal makes them brittle. It is undesirable, using fusion-welding processes if attempts are made to weld them because of the tendency to the crack formation, even though the use of the (Al-12 % Si) filler may sometimes give acceptable results. Solid-state techniques, such as friction stir welding may provide some success [7-10]. The weldability of (AA2024) by conventional fusion welding practices is limited. In addition, (AA2024) is more sensitive to cracking during conventional welding than other aluminum alloys [11, 12]. Reddy et al. [13] discussed the mechanical and corrosion properties of friction stir welded (7475-T761) aluminum alloy. The optimization process using Box Behnken Method of the process parameters was done with a minimum number of trials. They concluded that the Box Behnken Method had optimized the process parameters giving high joint efficiency. Verma et al. [14] studied the friction stir welding (FSW) of (7039) aluminum alloy. The trails are designed according to central composite design of response surface methodology (CCD-RSM). The optimization process has been done using desirability analysis. They concluded that the modelling was successfully done using the optimization process and the joint efficiency of the optimum condition is higher than that of the strength of the base material. Ghantas and Singhal [15] successfully welded of (AA7039-T6) aluminum alloy. The experiments were planned according to center composite design approach of response surface methodology (CCD-RSM). The optimization process of the process parameters was carried out using a hybrid approach of grey relation analysis. They concluded that the grey relational grade was improved with the predicted responses at the optimum conditions. However, there are some researches that have been done to discuss the single and multiple optimization process using different methods, no studies in the literature review have been particularly concerned with multiple optimization of (FSW) process using fuzzy logic-based desirability approach (Mamdani method).

2. The Taguchi Method

The Taguchi principle is most important method as compared with the other experimental design methods. Most limitations of this method are used for one single response only. Only the main control factors and the interactions between them are considered. In general, the Taguchi principle include, two important factors: (the control factor) and (the noise factor) which are usually used to study the effect of responses. The input factors are used to select the appropriate conditions for (FSW) process, whereas the noise parameters denote, all parameters that cause negative effects. Usually, the (S/N) ratio is determining for evaluating the single and multiple effect of the parameters and the maximum value can be used as the optimum value [16,17]. According to the quality outcomes, the (Taguchi) principle is divided into three major parts: the (Nominal-the-Better (NB)), the (Larger-the-Better (LB)) and the (Smaller-the-Better (SB)).

In this research, the following (Larger - the - Better (LB)) method is used in order to determine the higher response functions. The (S/N) ratios can be calculated as the following equation [18]:

$$SN_i = -10log\left(\frac{1}{N_i}\sum_{k=1}^{N_i}\frac{1}{y_k^2}\right) \quad (1)$$

Where: i, k, Ni stand for (number of experiments), (number of trials) and (total number of experiments), respectively.

3. Analysis of Variance (ANOVA)

The main objective of (ANOVA) is to determine which (FSW factors) significantly affect the quality characteristic. This is can be carried out by separating the total variations of the positive attributes, which is determined by the summation of the squared deviations from the total average of the positive attributes, into contribution percentage by each (FSW factors) and the error, as equations [19-21]:

$$SS_T = SS_F + SS_e \quad (2)$$

Where: $$SS_T = \sum_{j=1}^{p}\left(\gamma_j - \gamma_m\right)^2 \quad (3)$$

Where;

SS_T: Total squared deviations summation about the average.

γ_j : Average response for the (j^{th}) experiment.

γ_m: Total average of the response.

p: Number of experiments in the (Taguchi) array.

SS_F: Summation of squared deviations due to each parameter.
SS_e: Summation of squared deviations due to error.
The percentage contribution (P) can be calculated as [20]:

$$P = \frac{SS_d}{SS_T} \quad (4)$$

Where,
(SS_d): the sum of the squared deviations.

4. Multi-Objective Optimization Using Hybrid Approach (Desirability-Fuzzy Taguchi Experimental Design)

There are many statistical methods for solving multiple response problems like constrained optimization problems, overlaying the contours plot for each response, and desirability approach. The desirability method is favored due to its simplicity and availability in the software and gives flexibility in weighting and giving value for individual response. Solving these multiple response optimization problems by applying this technique includes combining multiple responses into a dimensionless value of performance named the multi-performance index (MPI).
In this research, the individual-desirability of all response (tensile strength and yield strength) is calculated with equation (4) [22]:

- For the one-sided transformation:

$$di = \begin{cases} 0 & \grave{y}_i \le y_i(\min) \\ \left(\frac{\grave{y}_i - y_i(\min)}{y_i(\max) - y_i(\min)}\right)^r & if\ y_i(\min) \le \grave{y}_i \le y_i(\max) \\ 1 & y_i(\max) \le \grave{y}_i \end{cases} \quad (5)$$

Weights are used to provide more importance on the upper/lower bounds or to highlight the target value. Weights can be extended between (0.1 and 1); a weight higher than (1) provides more importance on the goal, while weights less than (1) give less importance. The normalizing properties were determined according to the selection of quality characteristic of (tensile strength and yield strength) are larger the better. The computed individual desirability for each quality characteristics using the equation (5) [23]:

- For the two- sided transformation:

$$di = \begin{cases} \left\{\left(\frac{\grave{y}_i - y_i(\min)}{T_i - y_i(\min)}\right)^s\right\} & ,\text{if } y_i(\min) \le \grave{y}_i \le T_i \\ \left\{\left(\frac{\grave{y}_i - y_i(\min)}{T_i - y_i(\min)}\right)^t\right\} & ,\text{if } T_i \le \grave{y}_i \le y_i(\max) \\ \{0\} & \text{otherwise} \end{cases} \quad (6)$$

5. Experimental Setup

A vertical milling machine was used to weld the joints of similar (AA2024-T3) aluminum alloys. Figure 1 shows the arrangement of (AA2024-T3) plates on the machine during a welding process. Aluminum alloy plates with dimension of (200 × 100 × 3.5 mm) were used to make a butt joint. The tools rotate perpendicular to the longitudinal plate surface, which made of high-speed tool steel (HSS) with tapered pin profile, as shown in Figure 2.

Figure 1: Arrangement of (2024-T3) aluminum alloy plates

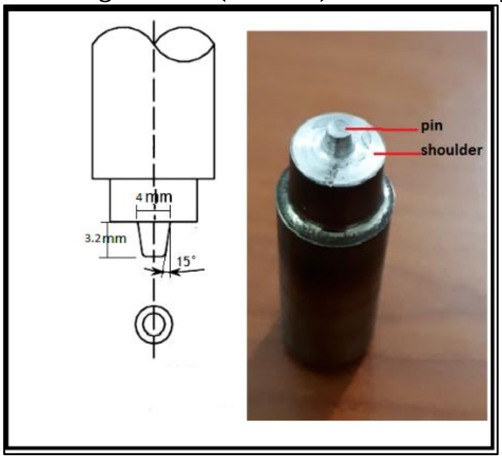

Figure 2: Fabricated tool

The chemical compositions and mechanical properties of alloy were carried out in the Department of Materials Engineering / University of Technology / Baghdad / Iraq, as shown in Table 1 and Table 2.

Table 1: Chemical composition of (AA2024-T3)

	Si	Fe	Cu	Mn	Mg	Cr	Zn	Ti	Al
Standard [24]	0.5	0.5	3.8-4.9	0.3-0.9	1.2-1.8	0.1	0.25	0.15	Rem.
Measured	0.677	0.429	0.309	0.0672	0.872	0.2	0.0132	0.112	Rem.

Table 2: Mechanical properties of (AA2024-T3)

	Tensile strength (MPa)	Yield strength (MPa)
Standard value [24]	434	289
Measured value	409	273

The tensile test specimens were cut perpendicular to the welding direction according to (ASTM B 557M – 02a) standard [25], as illustrated in Figure 3. The fractured samples of tensile test are shown in Figure 4.

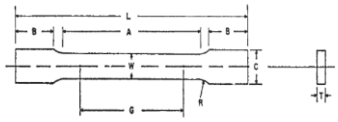

	Dimensions, mm	
	Standard Specimen Sheet-Type 12.5 mm Wide	Subsize Specimen 6 mm Wide
G—Gage length	50.00± 0.10	25.00 ± 0.10
W—Width (Note 1 and Note 2)	12.50± 0.05	6.01± 0.05
T—Thickness (Note 3)	thickness of material	thickness of material
R—Radius of fillet, min	12.5	6
L—Overall length, min (Note 4)	200	100
A—Length of reduced section, min	57	32
B—Length of grip section, min (Note 5)	50	30
C—Width of grip section, approximate (Note 2 and Note 6)	20	10

Figure 3: Standard dimensions of tensile test specimens [22]

Figure 4: Tensile fractured samples

6. Results and Discussion

I. Single-Objective Optimization of Tensile Strength and Yield Strength Using Taguchi Method

In this research, the experimental work was done according to (Taguchi) array. With respect to the experimental conditions, the number of levels and (FSW) parameters are given in Table 3, where (Taguchi) method, (L_{27}) array was employed. The (S/N) quantitative relation for tensile strength and yield strength can be calculated as (the Larger - the better) within the equation (1). The design array, including tests' values of tensile and yield strength, as shown in Table 4.

Table 3: Process parameters and their levels

Factor	Factor code	Levels		
		1	2	3
Shoulder diameter (mm)	A	12	14	16
Rotation speed (rpm)	B	710	1000	1400
Linear speed (mm/min)	C	40	56	80
Tilting angle (θ°)	D	1	2	3
Welding direction (Pass)	E	1	2	3

Table 4: The orthogonal array and experimental results of tensile strength and yield strength

No.	Shoulder diameter (mm)	Rotation speed (rpm)	Linear speed (mm/min)	Tilting angle (θ°)	Welding direction (Pass)	Tensile strength (MPa)	Yield strength (MPa)
1	12	710	40	1	1	205	205
2	12	710	40	1	2	211	210
3	12	710	40	1	3	217	217
4	12	1000	56	2	1	213	213
5	12	1000	56	2	2	218	217
6	12	1000	56	2	3	227	222
7	12	1400	80	3	1	256	214
8	12	1400	80	3	2	262	224
9	12	1400	80	3	3	271	237
10	14	710	56	3	1	224	222
11	14	710	56	3	2	233	227
12	14	710	56	3	3	241	231
13	14	1000	80	1	1	237	226

14	14	1000	80	1	2	245	231
15	14	1000	80	1	3	251	242
16	14	1400	40	2	1	308	261
17	14	1400	40	2	2	314	290
18	14	1400	40	2	3	326	298
19	16	710	80	2	1	95	87
20	16	710	80	2	2	110	109
21	16	710	80	2	3	116	112
22	16	1000	40	3	1	346	234
23	16	1000	40	3	2	353	247
24	16	1000	40	3	3	361	252
25	16	1400	56	1	1	292	286
26	16	1400	56	1	2	301	298
27	16	1400	56	1	3	308	301

Response graph method provided the output of interest to be optimized, i.e., minimize, maximize, targeted, etc. The output can be larger than one and it can be quantitative or qualitative. The factor effect of a parameter at any level is calculated by obtaining the mean of each (S/N) ratio at the same level. The graphical illustrations of factors influence at different levels are shown in Figure 5 and Figure 6 for tensile strength and yield strength, respectively.

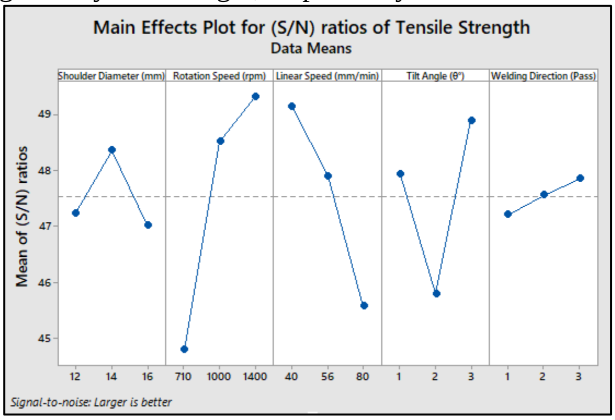

Figure 5: (S/N) values of tensile strength for aluminum alloy (2024-T3) joints at optimum condition

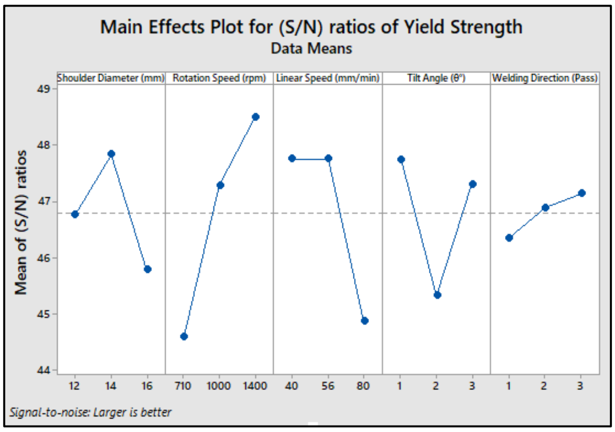

Figure 6: (S/N) values of yield strength for aluminum alloy (2024-T3) joints at optimum condition

The optimum tensile strength and yield strength values were at the higher (S/N) ratios in the response graphs. The optimum condition for tensile strength and yield strength becomes (A2B3C1D3E3) and (A2B3C1D1E3), respectively for main control factors, where the symbols (A, B, C, D and E) were explained in Table 3. Once the optimum parameters had been determined, the optimum performance of the response "tensile strength" at these parameters can be predicted. The predicted (S/N) ratio of tensile strength at optimum condition was calculated by adding the mean performance to the contribution of each parameter at the optimum level. The predicted results of tensile strength at the optimum condition are presented in Table 5.

Table 5: Predicted results of tensile strength at the highest (S/N) values

Taguchi Analysis: Tensile strength versus shoulder diameter, rotation speed, linear Speed, tilting angle and welding direction

Predicted values

S/N Ratio	Mean
53.4065	392.778

Factor levels for predictions

Shoulder Diameter (mm)	Rotation Speed (rpm)	Linear Speed (mm/min)	Tilt Angle (θ°)	Welding Direction (Pass)
14	1400	40	3	3

The final step of the single optimization process was the confirmation test, where the quality characteristics of the tensile strength can be obtained by applying the confirmation test within the optimum condition (A2B3C1D3E3). Table 6 shows the predicted and actual results at optimum level of each parameter to achieve the highest value of tensile strength. There is a good agreement between the predicted and experimental results of tensile strength.

Table 6: The predicated and actual values of tensile strength at the optimum condition

Tensile strength (predicted)		Tensile strength (actual)	
Mean	S/N	Mean	S/N
392.778	53.4065	388	52.8501
The optimum process condition			
Parameters level: A2B3C1D3E3			

The predicted results of (S/N) ratio and mean of yield strength at optimum condition are shown in Table 7.

Table 7: Predicted results of yield strength at the highest (S/N) values

Taguchi Analysis: Yield strength versus shoulder diameter, rotation speed, linear Speed, tilting angle and welding direction
Predicted values

S/N Ratio	Mean
51.7923	336.481

Factor levels for predictions

Shoulder Diameter (mm)	Rotation Speed (rpm)	Linear Speed (mm/min)	Tilt Angle (θ°)	Welding Direction (Pass)
14	1400	40	1	3

The confirmation test of yield strength was carried out at the optimum condition (A2B3C1D1E3), as shown in Table 8. The optimization process for yield strength test is successfully done using the method of Taguchi. According to these comparisons, the predicted and experimental values are in good agreement.

Table 8: The predicted and actual values of yield strength at the optimum condition

Yield strength (predicted)		Yield strength (actual)	
Mean	S/N	Mean	S/N
336.481	51.7923	268	49.8713
The optimum process condition			
Parameters level: A2B3C1D1E3			

(ANOVA) was used to analyze the effect of each parameter for tensile strength and yield strength, separately, as shown in Table 9 and Table 10 for tensile strength and yield strength, respectively.

Table 9: Analysis of variance (ANOVA) for tensile strength

General Linear Model: Tensile strength versus shoulder diameter, rotation speed, linear Speed, tilting angle and welding direction

Analysis of Variance

Source	DF	Adj SS	Adj MS	F-Value	P-Value
Shoulder Diameter (mm)	2	5171	2585.4	778.88	0.266
Rotation Speed (rpm)	2	60947	30473.4	9180.28	0.007
Linear Speed (mm/min)	2	35395	17697.3	5331.41	0.017
Tilt Angle (θ°)	2	21422	10711.1	3226.78	0.023
Welding Direction (Pass)	2	1120	560.1	168.74	0.986
Error	16	53	3.3		
Total	26	124108			

Table 10: Analysis of variance (ANOVA) for yield strength

General Linear Model: Yield strength versus shoulder diameter, rotation speed, linear speed, tilting angle and welding direction

Analysis of Variance

Source	DF	Adj SS	Adj MS	F-Value	P-Value
Shoulder Diameter (mm)	2	6098.3	3049.1	108.43	0.000
Rotation Speed (rpm)	2	34942.3	17471.1	621.30	0.000
Linear Speed (mm/min)	2	21083.6	10541.8	374.88	0.000
Tilt Angle (θ°)	2	9625.0	4812.5	171.14	0.000
Welding Direction (Pass)	2	1533.4	766.7	27.27	0.000
Error	16	449.9	28.1		
Total	26	73732.5			

From (ANOVA) table, the percentage of contribution of each parameter for tensile strength and yield strength can be obtained using the equation (4), as shown in Figure 7 and Figure 8 for tensile strength and yield strength, respectively.

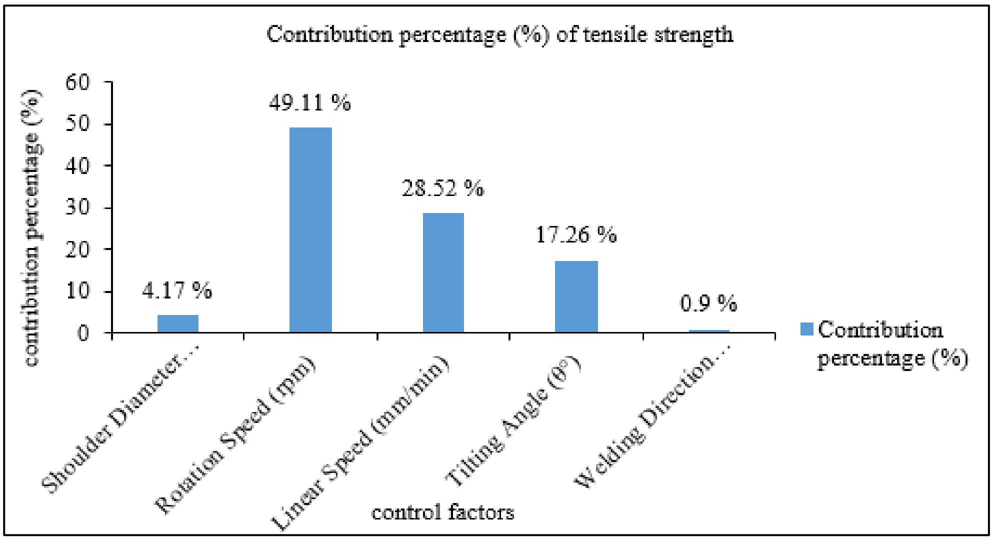

Figure 7: Percentages of contribution of tensile strength levels

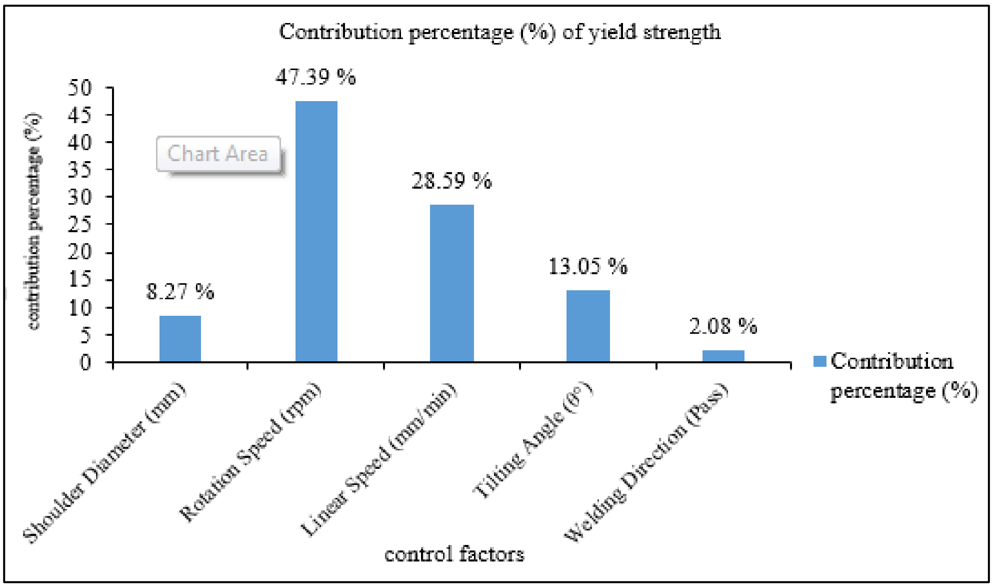

Figure 8: Percentages of contribution of yield strength levels.

II. Fuzzy logic proposed model

The present work uses a (Fuzzy Inference System - FIS) of (Mamdani) type to develop (membership function - MF) for input and output parameters use Matlab tool box software to obtain (MF) value using fuzzy operations, known as max-min reference method used for making of fuzzy rules. Mamdani receives all the individual normalized values of desirability as input and (MPI) values as output which are generated according to the (MF) and fuzzy rules. The essential steps included in the making of fuzzy model are fuzzification, fuzzy rules and defuzzification.

Fuzzification used to converts of crisp input values into imprecise (MF) such as small, medium, large etc. Triangular (MF) and fuzzy rules are established as Low, Medium and High. The low value and high value of the triangle were taken by equal intervals before and after the medium value. The output parameters are checked from rule viewer by changing the input parameters from low to high values by keeping the input parameters at different levels which are three fuzzy subset such as small (S), medium (M) and large (L), which is assigned to inputs (normalized output responses). The (MF) for input parameters is illustrated in Figure 9 and Figure 10 and Figure 11 for the output (MPI).

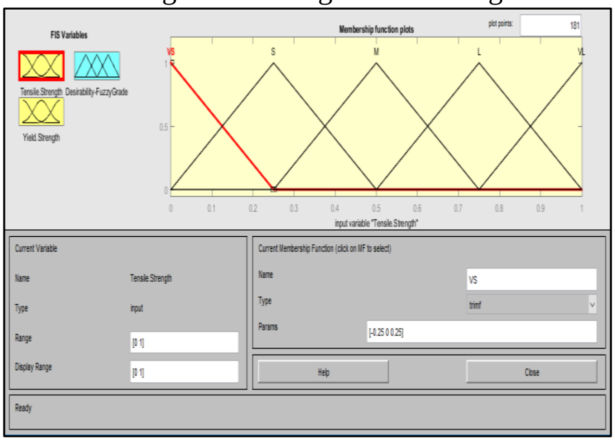

Figure 9: Membership plot for input parameter (tensile strength)

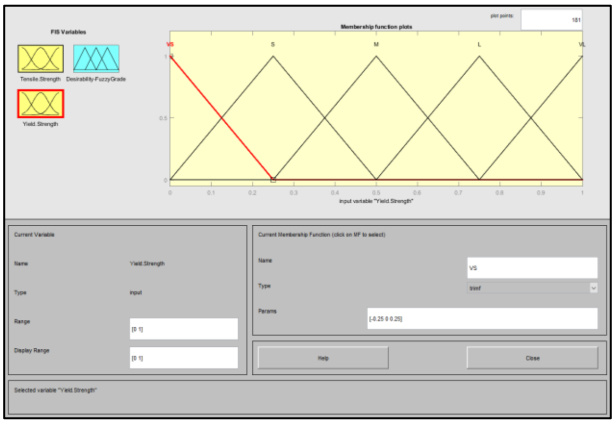

Figure 10: Membership plot for input parameter (yield strength)

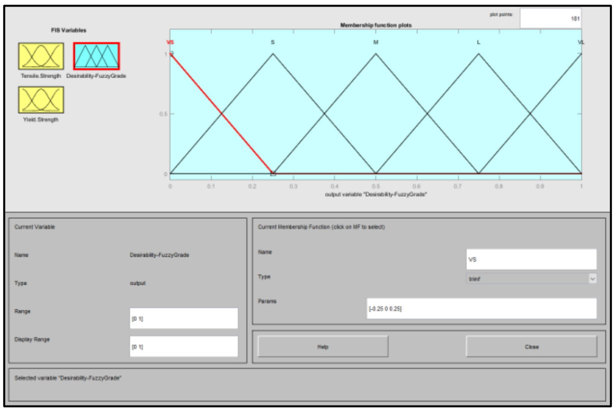

Figure 11: Membership plot for output (MPI)

The next stage of (FIS) is the relationship between the two parameters input (tensile strength and yield strength) and the one output (MPI) were described in the form of (if-then) control rules. Fuzzy rules are instantly made by the fact that "larger-the-better". Defuzzification involves the converts of fuzzy output into a crisp value. The centroid of the area is the most extensively used defuzzification technique. There are (27) rules taken based on the Taguchi design of the experiment. Thus, the multi-criteria optimization problem has been transformed into a single objective optimization problem by using the combination of utility theory fuzzy logic analysis.
The (S/N) ratios for (MPI) were determined based on the "higher-the-better," to maximize the responses. The (S/N) ratio for the response was calculated using equation (1). As shown in figure (12), the main effects plot (S/N) ratio is plotted for (MPI). Optimal (FSW) parameters setting are (A2B3C1D3E3), where the symbols (A, B, C, D and E) were explained in Table 3.

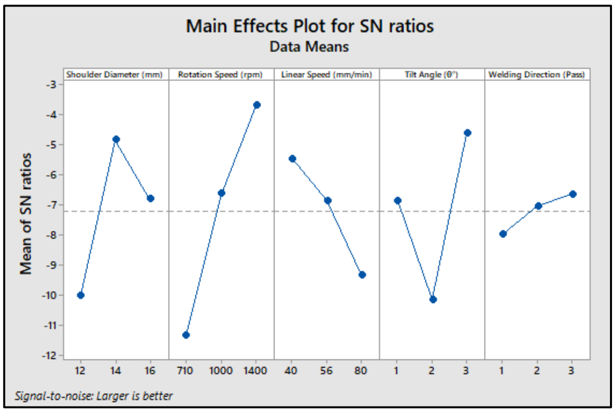

Figure 12: The (S/N) values of (MPI) for aluminum alloy (2024-T3) joints

For analyzing the significant effect of the process parameters on the response parameters, (ANOVA) was used. Table 11 shows the output of (ANOVA) analysis for (MPI), the table indicated the significance value of various input parameters. The contribution percentages of each control factor of (FSW) process for aluminum alloy (AA2024-T3) joints are shown in Figure 13.

Table 11: Analysis of variance (ANOVA) of (MPI) values

General Linear Model: Desirability Fuzzy-Grade (MPI) versus shoulder diameter, rotation speed, linear speed, tilting angle and welding direction

Analysis of Variance

Source	DF	Adj SS	Adj MS	F-Value	P-Value
Shoulder Diameter (mm)	2	0.36385	0.181926	108.81	0.000
Rotation Speed (rpm)	2	0.57429	0.287145	171.73	0.000
Linear Speed (mm/min)	2	0.19929	0.099645	59.60	0.000
Tilt Angle (θ°)	2	0.19929	0.099645	59.60	0.000
Welding Direction (Pass)	2	0.00736	0.003680	2.20	0.143
Error	16	0.02675	0.001672		
Total	26	1.37084			

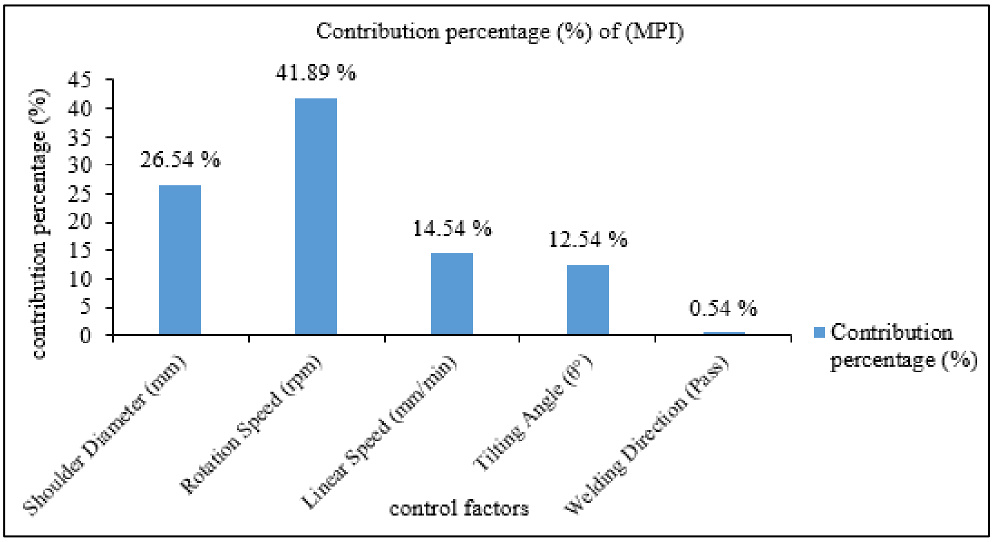

Figure 13: Percentage of contribution of the process parameters of (FSW)

III. Confirmation test

The improvement in predicted (MPI) at the optimum level is found to be large as compared with initial parameter setting (A2B3C1D3E3). The value of tensile strength and yield strength at this optimum level are shown in Table 12. The results of confirmation test show that two quality characteristics tensile strength and yield strength have been improved.

Table 12: Results of confirmation experiment for multi-objective optimization

	Initial	Optimized
Factor level	A1B1C1D1E1	A2B3C1D3E3
Tensile strength (MPa)	205	371
Yield strength (MPa)	198	268

IV. Characterization of welded samples

As mentioned in Table 5, the optimum condition (A2B3C1D3E3) "i.e. shoulder diameter (14 mm), rotation speed (1400 rpm), linear speed (40 mm/min), tilting angle (3°) and welding direction (3 passes)" was the best suitable to obtain a better joint.

The reasons behind the suitability of these parameters were that these parameters provided intense stirring of the material due to the proper shoulder diameter which generated good amount of heat to increase the ability of material to be mixed easily, and the high rotation speed with low linear speed helped the material to be mixed completely, as well as the tilting angle (3°) was permitted the

material to be mixed freedomly, and the three passes of welding helped to fill the voids and cracks that which could have existed during (FSW) process. These reasons led to finer grain structure and thus higher tensile strength and yield strength.
The microstructures of the cross-section for welded sample of (AA2024-T3 to AA2024-T3) at the optimum condition are shown in Figure 14. At the nugget zone, there was fine equiaxed grains. The grain size was changed by the strain rate and the heat input. From the experimental results, the finer grain size was produced by the higher heat input.

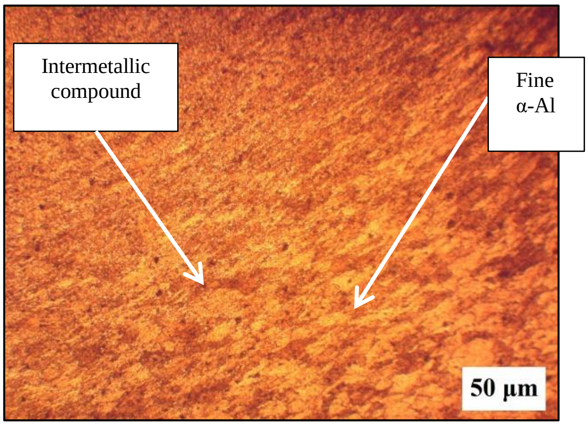

Figure 14: Microstructure of the welded (AA2024) at the optimum condition (shoulder diameter (14 mm), rotation speed (1400 rpm), linear speed (40 mm/min), tilting angle (3°) and welding direction (3 passes).

Scanning electron microscope (SEM) was used to characterize the fracture surface of (FSW) specimens after tensile testing. Fracture surface of the base material (AA2024-T3) after tensile testing, as observed under (SEM), is shown in Figure 15. Fine equiaxed dimples and hemispherical micro-voids were observed on the fractured surface. This indicated that the ductile failure occurred in the base material under tensile loading.

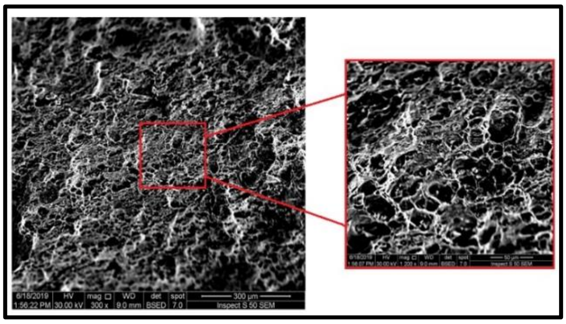

Figure 15: (SEM) image of the welded (AA2024) at the optimum condition (shoulder diameter (14 mm), rotation speed (1400 rpm), linear speed (40 mm/min), tilting angle (3°) and welding direction (3 passes).

(XRD) analysis results for parent alloy and (FSW) material were identical, and this indicated that there was no element depletion throughout (FSW) processes in this work. This result was however, expected because (FSW) was a solid-state process, and frequently, temperature throughout the joint was not high enough to induce phase transformation. This asserted what had been aforementioned just now. The (XRD) analysis is shown in Figure 16.

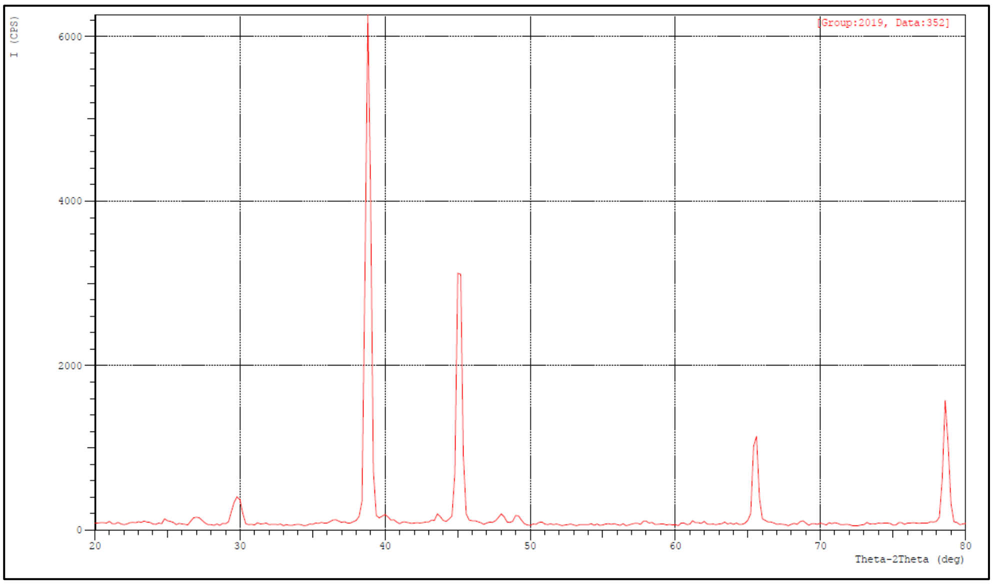

Figure 16: (XRD) analysis pattern of the welded (AA2024) aluminum alloy at the optimum condition (shoulder diameter (14 mm), rotation speed (1400 rpm), linear speed (40 mm/min), tilting angle (3°) and welding direction (3 passes)

7. Conclusion

In this research, it is thereby concluded that an improvement in mechanical properties for friction stir welded (AA2024-T3) by using multiple optimization method based on Taguchi method. The results of this investigation were: the single optimization by using (Taguchi method) showed the optimum condition for tensile strength was (365 MPa) and for yield strength was (258 MPa), at the parameters: shoulder diameter (14 mm), rotation speed (1400 rpm), linear speed (40 mm/min), tilting angle (3 degree) and welding direction (3 passes). The multi-response optimization for (FSW) process at the optimum condition for tensile strength and yield strength were (371 MPa) and (268 MPa), respectively; at the parameters: shoulder diameter (14 mm), rotation speed (1400 rpm), linear speed (40 mm/min), tilting angle (3 degree) and welding direction (3 passes). The rotation speed is the most significant variables of the optimum outcome results with major influence (41.89 %) of the (FSW) process, followed by shoulder diameter with (26.54 %) effects on the response parameters.

References

[1] A. M. Eramah, M. P. Rakin, D. M. Veljic, S. Tadic, N. A. Radovic, M. Zrilic and M. M. Peroviv, “Influence of friction stir welding parameters on properties of (2024-T3) aluminum alloy joints,” Thermal Science, Vol. 17, No. 1, pp. S21-S27, 2013.

[2] A. A. Zainulabdeen, “Investigation of fatigue properties of dissimilar aluminum joints by friction stir welding,” PhD Thesis, University of Technology/ Department of Production Engineering & Metallurgy-Iraq, 2013.

[3] R. Nunes, “Properties and selection: Nonferrous alloys and special-purpose materials,” ASM Handbook, Vol. 2, Edition 10, 1992.

[4] J. M. S. AL-Murshdyand and Q. K. N. Chabuk, “Effect of Tool shape geometry and rotation speed in friction stir welding of (2024-T3),” The Iraqi Journal for Mechanical and Material Engineering, Vol. 16, No. 3, 2016.

[5] A. M. A. Al-Doori, “Fatigue Properties of Friction Stir Welded Aluminum Alloys,” M.Sc. Thesis, Al-Nahrain University/ College of Engineering, Baghdad-Iraq, 2010.

[6] N. K. Srinivasan, “Welding technology,” Khanna Publishers Delhi-India, 2008.

[7] D. Trimble, H. Mitrogiannopoulos, G. E. O’ Donnell and S. McFadden, “Friction stir welding of (2024-T3) plate - the influence of different pin types,” Mechanical Sciences., Vol. 6, No. 1, pp. 51-55, 2015.

[8] S. A. Khodir, T Shibayanagi and M. Naka, “Microstructure and mechanical properties of friction stir welded (AA2024-T3) aluminum alloy,” Materials Transactions, Vol. 47, No. 1, pp. 185-193, 2006.

[9] G. Mathers, “The welding of aluminum and its alloys,” Cambridge press (CRC), 2002.

[10] Lamet, “Welding, brazing and soldering,” ASM Handbook, Vol. 6, 1993.

[11] M. L. Saad, “The effect of tool geometry on the strength of (AA2024-T3) of friction stir welding,” M.Sc. Thesis, Middle Technical University - Iraq, 2015.

[12] R. S. Parmar, “Welding engineering and technology,” Khanna Publishers Delhi-India, 4th Edition, 2005.

[13] S. A. N. J. Reddy, R. Sathiskumar, K. G. Kumar, S. Jerome, A. V. Jebaraj, N. Arivazhagan and M. Manikandan, “Friction based joining process for high strength aerospace aluminium alloy,” Materials Research Express, Vol. 6, No 8, 2019.

[14] S. Verma, M. Gupta and J. P. Misra, “Optimization of process parameters in friction stir welding of armor-marine grade aluminium alloy using desirability approach,” Materials Research Express, Vol. 6, No. 2, 2018.

[15] G. Ghangas and S. Singhal, “Modelling and optimization of process parameters for friction stir welding of armor alloy using RSM and GRA-PCA approach,” Mater. Res. Express, Vol. 6, 2019.

[16] M. Beaver, “Introduction to probability and statistics,” Cengage Learning, 4th edition, 2013.

[17] A. K. Hussein, L. K. Abbas and J. J. Dawood, “Multiple objective optimization of weld geometry of dissimilar metals,” The Iraqi Journal for Mechanical and Material Engineering, Vol.16, No. 4, 2016.

[18] H. Singh, “Taguchi optimization of process parameters: a review and case study,” International Journal of Advance Engineering Research and Studies, Vol. 1, No. 3, pp. 39-41, 2012.

[19] D. C. Montgomery and G. C. Runger, “Applied statistics and probability for engineers,” John Wiley, 5th edition, 2012.

[20] E. K. Zavadskas, A. Zakarevicius and J. Antucheviciene, “Evaluation of ranking accuracy in multi-criteria decisions,” Iformatica, Vol. 17, No. 4, pp. 601-618, 2006.

[21] N. Parandin and M. A. F. Araghi, “Ranking of fuzzy numbers by distance method,” Journal of Applied Mathematics, Islamic Azad University of Lahijan, Vol. 5, No. 19, 2008.

[22] R. S. Rama and G. Padmanabhan, “Application of taguchi methods and (ANOVA) in optimization of process parameters for metal removal rate in electrochemical machining of (Al/5 % SiC) composites,” International Journal of Engineering Research and Applications (IJERA), Vol. 2, No. 3, pp. 192-197, 2012.

[23] A. K. Hameed, “Multiple response optimizations of carburized steel,” M.Sc. Thesis, University of Technology/ Department of Materials Engineering-Iraq, 2013.

[24] American Society for Testing and Materials (ASTM) “Standard specification for aluminum and aluminum alloy sheet and plate,” ASTM B 209-96, 1996.

[25] ASTM B 557 M-02a, “Standard test methods of tension testing wrought and cast aluminum- and magnesium-alloy products (metric),” 2008.